Mine Water and the Environment (2021) 40:298–307
https://doi.org/10.1007/s10230-020-00709-3

TECHNICAL ARTICLE

Assessment of Tailings Ponds by a Combination of Electrical (ERT and IP) and Hydrochemical Techniques (Linares, Southern Spain)

J. Rey[1] · J. Martínez[2] · M. C. Hidalgo[1] · R. Mendoza[2] · S. Sandoval[3]

Received: 20 January 2020 / Accepted: 20 August 2020 / Published online: 1 September 2020

Abstract

Accumulated mine waste in certain locations in the abandoned mining district of Linares-La Carolina (southern Spain) contain high levels of metals. Therefore, in recent years, many of these tailings ponds have been restored and sealed. This study assessed the efficacy of two geophysical techniques, electrical resistivity tomography (ERT) and induced polarisation (IP), combined with hydrochemical studies, as tools to image the effectiveness of the encapsulation. In the bedrock, ERT profiles distinguished a surficial layer of moderate-low resistivity values (below 80 Ω m), associated with alluvial sands or altered granite, and a deeper zone of high resistivity (up to 1000 Ω m) related to unaltered granite basement. Lateral changes in resistivity were identified inside the upper layer and downstream of the tailings pond. The IP profiles detected local anomalies in the chargeability values (up to 8 mV/V), unusual in granitic rocks. The locations with high chargeability also had low resistivity, which typically indicates the percolation of mining leachates in the underlying altered granites. Integration of geological and geochemical information confirmed this interpretation. This work verified that the combined use of ERT and IP methods were effective for monitoring ancient tailings ponds and for assessing tailings encapsulation.

Keywords Mine waste · METAL(loid) · Leachate detection · Resistivity · Chargeability · Environmental quality

Introduction

Underground mining of metallic sulfide ores have produced, through centuries of extractive activities, great amounts of accumulated wastes (waste rock, floating sludge, smelter slag, etc.). Although relatively recent regulations promote a more environmentally sustainable way of exploiting natural resources, in most cases, these modifications do not address abandoned mines, which are important pollution sources (Bundschuh et al. 2012; Ji et al. 2013). As a result, such sites have supplied, and in many cases continue to contribute, contaminants to the surrounding soil and nearby water bodies, decades after a facility's closure. This is a worldwide problem (Bundschuh et al. 2012; Gratton et al. 2000; Herbet 1997; Yun et al. 2016).

This situation has been identified in the Linares-La Carolina mining district (southern Spain, Jaén Province, Fig. 1a) (Martínez et al. 2008, 2016). This mining district is characterised by vein deposits, mainly composed of galena (PbS). The area was subjected to intense mining, which was abandoned at the end of the 1970s. This underground mining activity produced a large amount of mine wastes, which were deposited nearby. In addition, the tailings from mineral concentration processes, specifically waterborne refuse material, were deposited without any soil preconditioning. Sulfides, present in flotation tailings, are unstable under the weathering conditions to which they are exposed and adversely affect the environment (Chopin and Aloway 2007; Li and Thornton 2001; Sobanska et al. 2000). The oxidation of these sulfide minerals results in the formation of sulfates, a decrease in water pH, and the release of metal(loid)s, such as As, Fe, Mn, Pb, and Zn into solution (Moncur et al. 2005; Nordstrom et al. 2015). Acid generated during the oxidation of sulfides can be neutralised by the dissolution of carbonate, hydroxide, and silicate minerals,

✉ J. Rey
jrey@ujaen.es

[1] Dpto. de Geología, EPS de Linares and CEACTEMA, Universidad de Jaén. Campus Científico Tecnológico, 23700 Linares, Jaén, Spain

[2] Dpto. de Ingeniería Mecánica y Minera, EPS de Linares and CEACTEMA, Universidad de Jaén. Campus Científico Tecnológico, 23700 Linares, Jaén, Spain

[3] Everest Geophysics SL, Cosme Gamella 23, Colmenarejo, 28270 Madrid, Spain

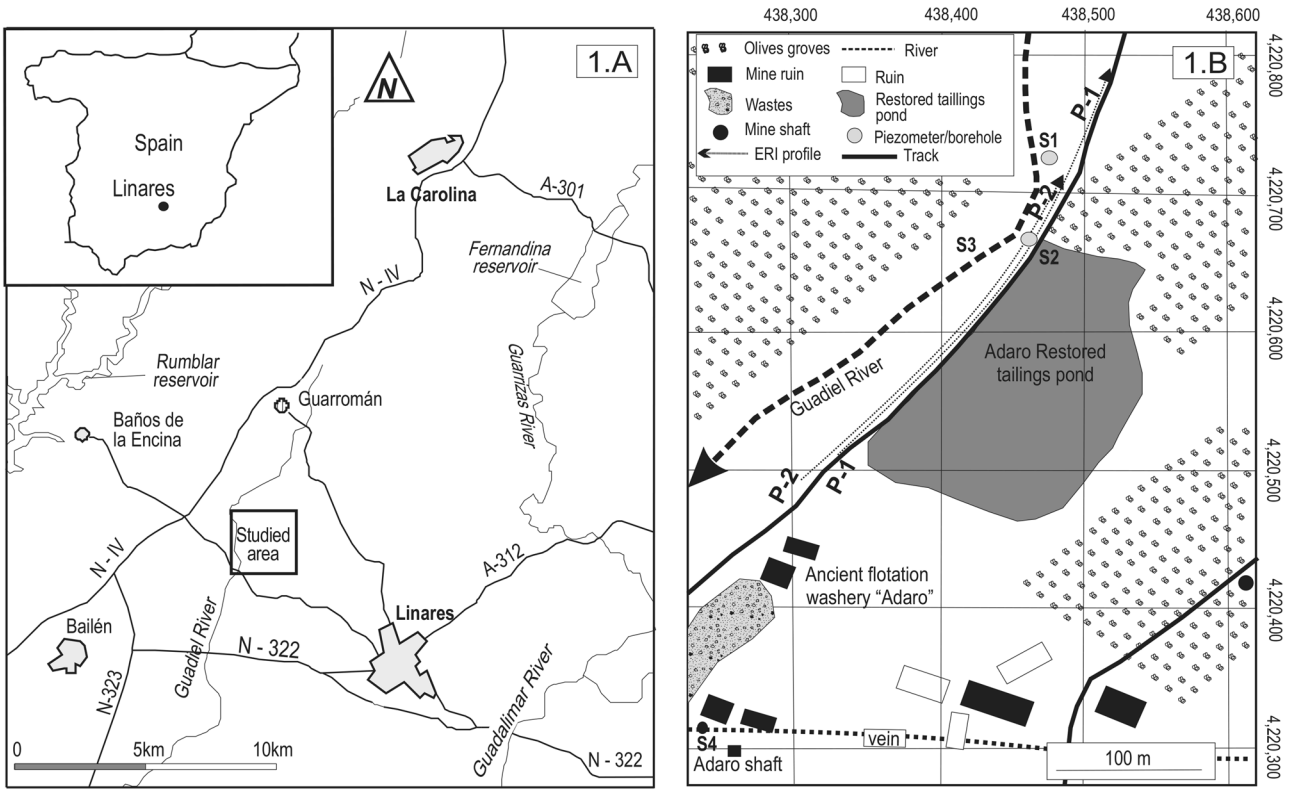

Fig. 1 **a** Geographical location of the study area. **b** Position of the electrical tomography profiles and water sampling points. Electrical tomography profiles: P-1 and P-2. Hydrochemical sampling points: borehole near the Guadiel River (S1), piezometer near the tailings pond (S2), the Guadiel River (S3), and the Adaro shaft mine (S4)

resulting in the occurrence of neutral mine drainage. When sufficient neutralisation capacity is available within mine wastes, leachate pH remains circumneutral, but the water can still contain metal(loid)s that exceed regulatory water pollution standards (El Adnani et al. 2016; Lindsay et al. 2015; Navarro et al. 2015).

In the Linares district, after the passing of regional environmental laws, regional authorities closed down and restored various abandoned mining waste deposits. The goal of the proposed actions was to stabilize the deposits physically and chemically to guarantee their structural safety and prevent pollution. The objective of this study was to determine whether two geophysical prospecting techniques (electrical resistivity tomography (ERT) and induced polarisation (IP)) could be used to assess the efficacy of these techniques by detecting leachates and analysing possible effects on underlying bedrock. This methodology for the structural analysis of tailings ponds and the verification of seal effectiveness could be extrapolated to other mining regions with similar problems.

Description of the Study Area

Geological and Mining Background

Geologically, two groups of materials can be differentiated in the study area: a Palaeozoic basement and an underlying subhorizontal post-Hercynian cover (Azcárate 1977; Lillo 1992). The Palaeozoic basement is composed of metamorphic rocks (basically phyllites interspersed with quartzites), which were intensely deformed during the Hercynian orogeny and affected by a granitic intrusion. The tectonics produced a considerable network of fractures in the region, with two predominant directions: N25° E and N80° E. Many of these fractures were mineralised by hydrothermal flows rich in Pb–Ag sulfo-antimonides and Cu–Fe sulfides. These veins have historically been the target of intense underground mining, but were abandoned during the late 20th century.

The mineralogical industry developed in parallel with the creation of numerous gravimetric and flotation plants. Until the mid-1950s, only gravimetric techniques were used to differentiate ore and waste rock. The waste products were typically deposited in heaps located near the mining facilities, sometimes possessing high mineral grades due to the

technical limitations of these processes (Gutiérrez-Guzmán 1999).

During the second half of the 20th century, a flotation process was introduced to separate and concentrate metal-bearing minerals in the Linares-La Carolina mining district. The final waste products were deposited in tailings ponds, often with no prior land preparation. This practice created considerable environmental risks. At least 32 large tailings impoundments have been identified in this mining district (Gutiérrez-Guzmán 1999). Significant attention is currently given to the management of these potentially hazardous materials.

Despite the sulfide mining, the Linares abandoned mining district is characterised by neutral mine drainage (Hidalgo et al. 2006, 2010). In most of the mines, metal(loid)s are barely mobilised in waters pumped from the flooded voids, which are characterized by net alkaline pH values (from 6.7 to 8.2). The ore veins are hosted in a granitoid massif and consist of sulfide mineralisation with abundant carbonate gangue (mainly calcite and ankerite). This association of carbonate rocks with the metallic ores neutralise any acid that forms by the oxidation of sulfide minerals. Nevertheless, these mine waters are enriched in sulfate and calcium (compared with groundwater from the host granitoid), and, in certain cases, remarkable levels of Fe and Mn.

The Adaro Area

This study was conducted near Linares, in the Adaro area (Fig. 1). This area contains a large, 160 m long, 120 m wide, and 35 m high raised tailings pond, with an estimated waste volume of 300,000 m^3. The mineralogy of the tailings was studied by De la Torre et al. (2012), before the restoration of the mine pond. The tailings are mainly composed of quartz (30-35%), accompanied by phyllosilicates (25–30%), and feldspar, calcite, and ankerite, classified as abundant (10–15%). Galena, cerussite, and lepidocrocite also appear, but only as trace minerals (< 5%). The total contents of 24 metal(loid)s were also analysed (Rojas et al. 2012): the concentrations were quite similar in surface and bottom samples, and significant values were found for Fe (25,600–26,900 mg/kg, surface-bottom), Pb (3400–1200 mg/kg surface-bottom), Zn (150–100 mg/kg surface-bottom), and As (35–38 mg/kg surface-bottom).

This structure was restored and sealed in 2011 (Fig. 1b). Figure 2 shows several photographs of this structure. The first photograph (Fig. 2a), taken in the 1970s before the restoration and sealing process, shows the formation of gullies, through which tailings were carried to the Guadiel River. The second photograph, taken in 2016 (Fig. 2b) shows the current state after restoration (placement of a retaining wall in the lowest part, intermediate berms, and a seal).

Sealing was performed using in situ encapsulation techniques through waterproof barriers (García-Fernández and Gallego 2009) in addition to surface runoff control and groundcover restoration (Figs. 2b–d). Figure 2e includes a cross-section of the restored tailings pond. Cortada et al. (2017) used ground penetrating radar (GPR) technology to detect possible discontinuities in the geotextile layers used to waterproof the pond, which could have influenced the effectiveness of the sealing process.

In the Linares-La Carolina mining district, the internal characterisation of mining dams was performed with ERT (Cortada et al. 2017; Martínez et al. 2012, 2016). ERT has been used in other mining areas (Martín-Crespo et al. 2015; Martínez-Pagán et al. 2009; Zarroca et al. 2015), where the generated resistivity models have identified the morphology of the structures, variations in the vertical and horizontal distributions of the deposited materials, the contacts of mining wastes with the substrate, and fracture zones in the bedrock. However, resistivity variations can occur due to different parameters: changes in lithology, water content, and pore fluid chemistry (Power et al. 2018; Puttiwongrak et al. 2019; Slater and Lesmes 2002). To avoid uncertainties, ERT and IP were both used, and the results were compared with physico-chemical parameters measured in groundwater sampled at nearby piezometers and boreholes.

Materials and Methods

Electrical Resistivity Tomography (ERT)

This geophysical prospecting technique determines the distribution of electrical resistivity in the subsoil as described by Telford et al. (1990). The development of automatic data acquisition systems (multi-electrode resistivity meters) and, above all, appropriate software for rapid information processing has accelerated the application of geoelectric resistivity methods for solving complex geological models. Accordingly, ERT has emerged as one of the most effective non-invasive tools for subsoil analysis and characterisation.

ERT involves placing numerous electrodes along a profile (or a mesh in 3D studies), at a constant distance from each other. The separation and total number of electrodes determines the resolution of the survey and the maximum investigation depth, respectively. In ERT, the closer the electrodes are, the higher the resolution, while the farther apart they are, the greater the penetration depth (Sasaki 1992). Another parameter that strongly influences the vertical and horizontal resolution and the penetration depth is the measuring configuration, also known as the "quadripole array". This configuration describes a combination in which four electrodes are used for every single measurement. For a

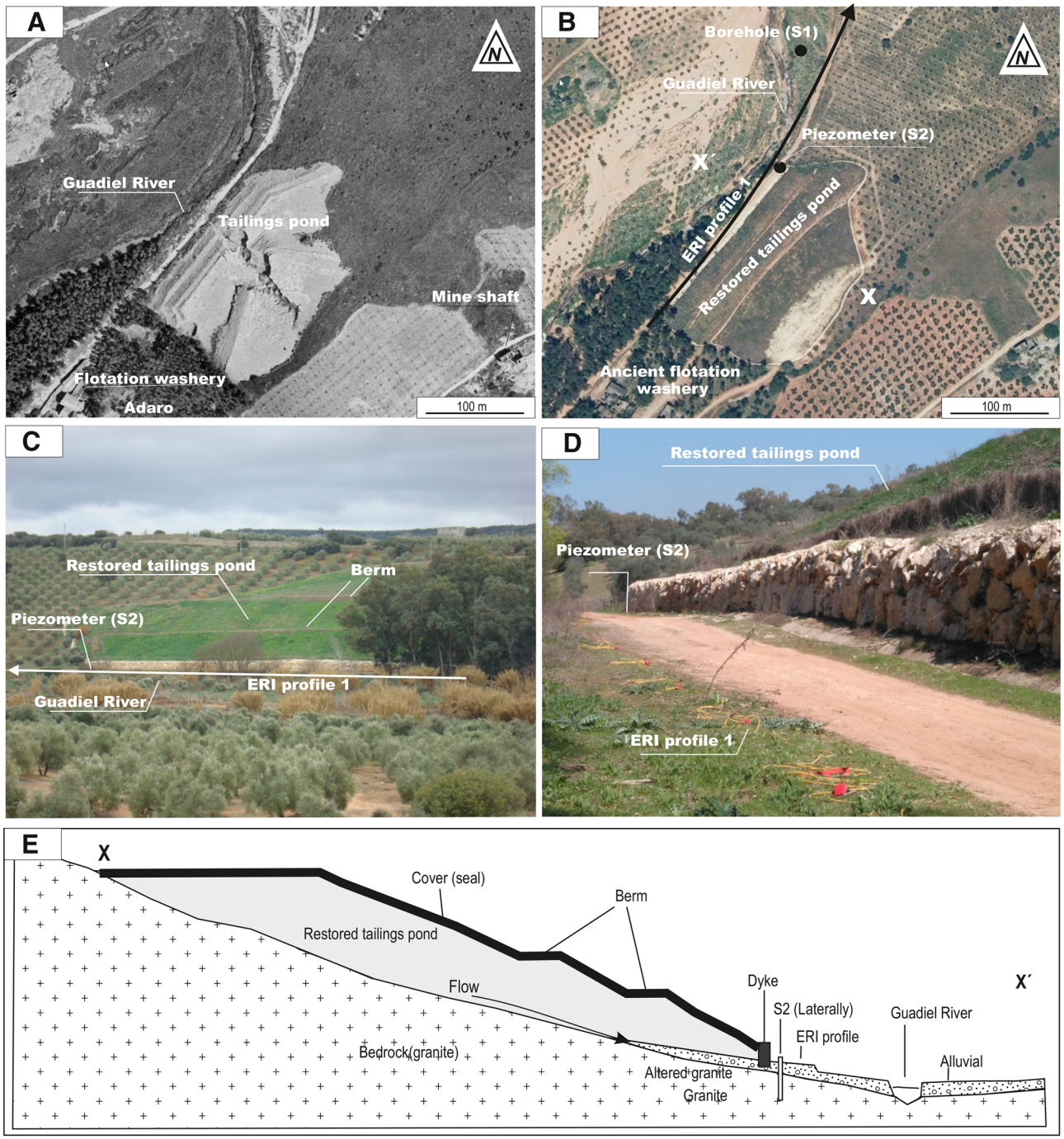

Fig. 2 **a** Aerial photograph of the tailings pond taken in the 1970s when the Adaro mine was in operation, showing the existing gullies. Eroded material was directly transferred to the Guadiel River. **b** Aerial photograph taken in 2016 showing the restored tailings pond and the positions of the piezometer, the borehole and the cross-section (X–X´). **c** Restored tailings pond and position of the tomography profile P-1. **d** Detail of the bottom of the restored tailings pond and the positions of the P-1 profile and piezometer S2. **e** Cross-section of the restored tailings pond

thorough description on ERT arrays, we refer the reader to Telford et al. (1990).

In this study, two ERT profiles were acquired, one with 80 electrodes and the other with 64 electrodes, 5 m apart (Figs. 1b, 2c, d), with total lengths of 395 m and 315 m, respectively. For the first profile, a Wenner-Schlumberger array was used. This array is moderately sensitive to both horizontal and vertical features. In areas where both types

of geological structures are expected, this array might be a good compromise between the Wenner and the dipole–dipole array (Dahlin and Zhou 2004; Loke 2014).

The second profile was recorded using a dipole–dipole array. This array is very sensitive to lateral changes in resistivity, but is relatively insensitive to vertical resistivity changes. This contrast means that the array is good for mapping vertical structures, such as dykes and cavities, but relatively poor for mapping horizontal structures, such as sills or sedimentary structures (Dahlin and Zhou 2004; Loke 2014). The simultaneous use of two devices allowed the two results to be compared so that we could determine which was more effective for tailings ponds assessment.

The electrical tomography equipment utilized was a RESECS model by Deutsche Montan Technologie (DMT). The ERT profiles were interpreted from the apparent resistivities assessed during the field work, which were treated using the specific software RES2DINV (Loke and Barker 1996). This calculation software is based on the least-squares method with dampl smoothing, modified with the quasi-Newton optimization method. The inversion method constructs a subsoil model using rectangular prisms and determines the resistivity values for each prism, minimizing differences between observed and calculated apparent resistivity values (Loke and Barker 1996; Loke and Dahlin 2002).

Induced Polarisation (IP)

With IP, a continuous electrical current of a specific intensity is injected into the terrain and generates a voltage. When the current is switched-off, the voltage drops gradually (Sumner 1976; Telford et al. 1990). The voltage decay curve is recorded during a specific interval. The apparent chargeability is defined as the area under the voltage decaying curve between two instants divided by the original potential Vo (Binley and Kemna 2005; Zhadanov 2018).

Geophysical prospecting with IP has been used to test oil wells (Telford et al. 1990) and to locate metal deposits (Bery et al. 2012; Fadele et al. 2018; Irawan et al. 2013; Martínez et al. 2019; Moreira et al. 2014) as well as in hydrogeology (Towel et al. 1985). In recent years, geophysical prospecting has also been successfully used in environmental studies (Slater and Lesmes 2002), to detect hydrocarbon-contaminated plumes (Blondel et al. 2014; Deceuster and Kaufmann 2012; Schwartz and Furman 2012) and analyse industrial waste disposal sites (Aristodemou and Thomas-Betts 2000). In this study, a detailed profile of the tailings pond was obtaining using 64 electrodes placed 5 m apart, with a total length of 315 m, which matched the resistivity profile 2 (Fig. 3). A dipole–dipole array was also used.

Modern resistivity meters can measure apparent resistivity and chargeability simultaneously. These kind of surveys require the use of non-polarising electrodes because they offer greater stability in the measurements and reduce polarisation effects when prolonged injections of current are required. The electrode is filled up with Pb chloride saturated in hard gel and an inner spiral core. The current injection time and switch-off delay were 1024 and 120 ms, respectively, and the interval between measurements was 1 s.

The apparent resistivity and chargeability measurements were treated using the software PROSYSII and subsequently analysed using the software RES2DINV, which is specific for resistivity and IP (Griffiths and Barker 1993; Loke and Barker 1996).

Hydrochemistry

Groundwater samples were collected from a 90 m deep borehole located near the Guadiel riverbed, upstream of the restored pond (S1 in Fig. 1b). In addition, a 10.5 m deep piezometer located in the lowest part of the pond (S2 in Fig. 1b), which had been installed in a borehole drilled during the restoration work, was subsequently used for water quality monitoring. The borehole and the piezometer were purged with a portable pump before sampling. Water samples were obtained at different depths using a point-source sampling bailer.

Furthermore, surface water samples were collected from the river (Guadiel River, S3 in Fig. 1b) and from the Adaro shaft mine, which is currently flooded (S4 in Fig. 1b). The shaft has been used for the last 20 years as a pumping well to obtain water for irrigation. Water samples were collected after 15–20 min of pumping, when the temperature and electrical conductivity (EC) of the water had stabilized.

In all cases, temperature, EC, and pH were determined in situ. Temperature and pH were measured using a Hach Lange HQ20 portable pH meter and a portable conductivity meter WTW LF92 with automatic temperature compensation was used to measure the EC. In addition, well logging was performed in borehole S1 using a water quality probe, with different electrodes continuously reading various parameters (EC, temperature, pH, redox potential, and dissolved O_2).

Water samples collected for metal(loid) analysis were filtered in the field using a 0.45 µm filter. The samples were preserved by adding ultrapure nitric acid to pH < 2.5 and by maintaining them cooled during transport to the laboratory. Analytical tests were performed at the Central Research Support Services laboratories of the University of Jaén. The techniques used were bicarbonate titration and ionic chromatography (Metrohm Compact IC Flex)

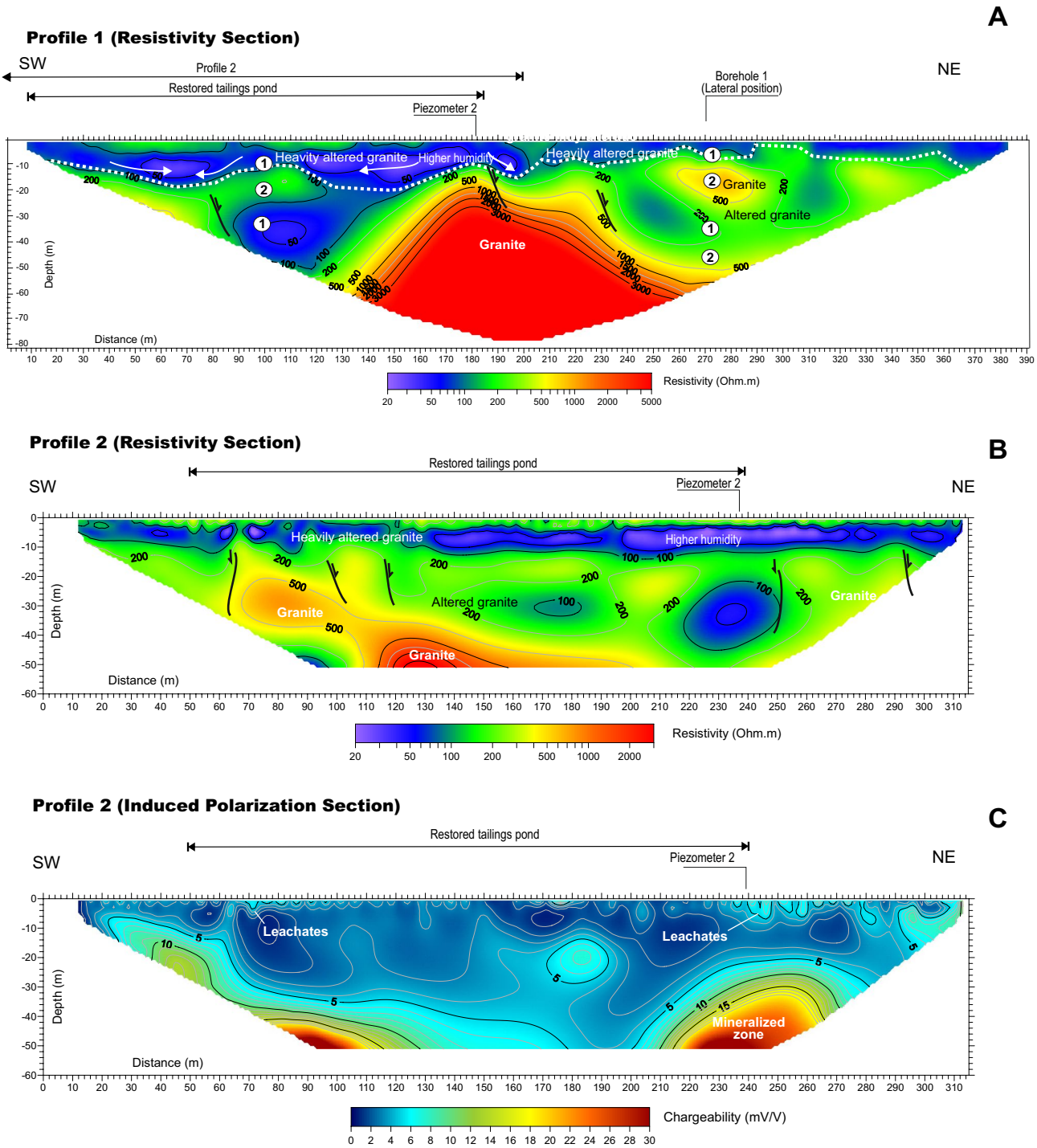

Fig. 3 **a** Electrical tomography profile P-1. 1: low-resistivity zone; 2: medium-to-high resistivity zone. **b** Electrical tomography profile P-2. **c** IP profile P-2

for major and minor constituents and inductively coupled plasma mass spectrometry (ICP-MS Agilent 7500a) for trace elements. As a quality control measure, samples were analysed in duplicate using certified high purity standards and reference blanks.

Discussion and Results

Electrical Resistivity Tomography (ERT)

Figures 1b and 2b show the location of ERT profile 1 obtained in the lowest part of the tailings pond, in the

SW-NE direction. In the data inversion process, 5 iterations were performed with a 6.4% root mean square (RMS) error. The true resistivity profile shows two large vertical sets (Fig. 3a). The more superficial of the sets, with low values (all less than 80 Ω.m) is associated with alluvial sands or highly altered granite (the two lithologies are difficult to differentiate). The other set is found at the bottom of the profile and is characterised by increased resistivity (which can exceed 1000 Ω.m). This set is associated with moderately altered granite. Resistivity values are not uniform in the bedrock. Therefore, within this set, zones with lower (1 in Fig. 3a, associated with fractured/altered granite) and higher (2 in Fig. 3a, linked to a less altered granite) resistivities can be differentiated.

Lateral changes in resistivity values are also detected in the top set. Therefore, the resistivities of the upper layer, consisting of sands/highly altered granite, are approximately 20–40 Ω.m in the first half of the profile (towards the SW), while resistivities can reach 80 Ω m in the second half of the profile (towards the NE). The decrease in resistivities coincides with the upstream tailings pond and potentially indicate the presence, in some small areas, of mining leachates with high concentrations of salts and metal(loid)s, thereby suggesting that the waterproofing process was not as effective as desired.

Figure 4 shows the drilling column of piezometer S1 and some of the parameters assessed in the well logging (conductivity and pH). For the first 15 m, consisting of sand and highly altered granite, unaltered and compact granite intersects the profile, followed by a zone of highly altered granite at depths from 48 to 52 m. Although the ERT profile does not intersect the piezometer, which is ≈ 20 m away, this column and the electro-facies interpretations correlate perfectly (compare Figs. 3a and 4).

Profile 2 (Fig. 3b), shorter than profile 1 for greater detail, was obtained directly along profile 1. Figure 3a shows the relationship between the two profiles. In the inversion process for profile 2, four iterations were performed, reaching a 4.8% root mean square (RMS) error.

Although, as previously mentioned, different arrays were chosen (the first was a Wenner–Schlumberger array, and the second was a dipole–dipole array), in general, the results were very similar. In the more detailed profile, within the top set of low resistivities, which is under the dam, the NE sector has the lowest values, which can be associated with the presence of mining leachates. The existence of leachates in this zone was confirmed by hydrochemical analysis of the water collected at piezometer 2.

At great depths, less resistive zones were found in the granite under the pond, especially on the NE bank of the tailings pond, where the resistivity in the granite was ≈ 20 Ω.m at depths of 20–40 m. At the SW end, at a depth of 50 m, a sharp drop in resistivity was also detected, with values less than 20 Ω m.

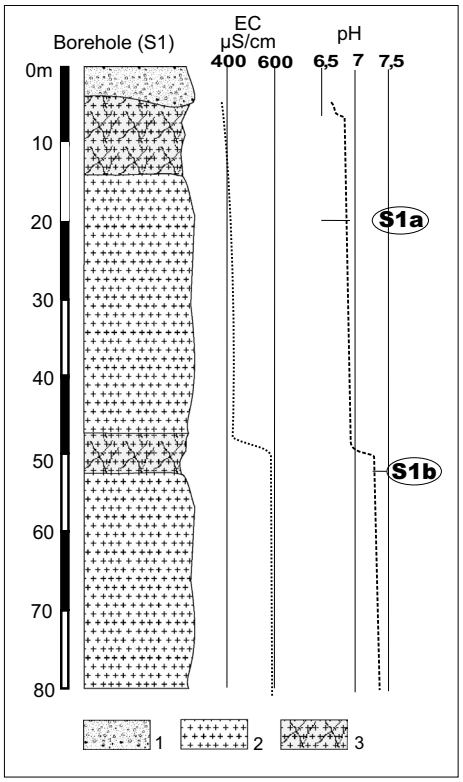

Fig. 4 Drilling column in the piezometer (S1) near the Guadiel River. Electrical conductivity (EC) and pH logs, measured using the water quality probe, are indicated in the figure, with the positions of the collected water samples (S1a and S1b). 1: loose material (sands); 2: highly altered granite; 3: unaltered granite

In general, comparing the data from the Wenner-Schlumberger (Fig. 3a) and dipole–dipole arrays (Fig. 3b) confirms that the lateral resistivity changes were identified better by the dipole–dipole array. This second device, was better able to detected more abrupt resistivity variations, which may be related to the presence of fractures. These structures generate secondary porosity that creates preferred areas for underground flow (Fig. 3b).

Induced Polarisation (IP)

The IP profile (Fig. 3c) matches that of resistivity profile 2 in Fig. 3b. In this case, in the data inversion process, four iterations were performed with a 2.1% root mean square (RMS) error.

From an in-depth analysis of the first 20 m, low values of chargeability were detected, i.e. generally less than 1 mV/V, which is common in granitic rocks (Fadele et al. 2018; Loke 2014), and no evidence of leachate contamination was detected. The chargeability only increases in the top section,

at both ends of the pond, reaching 8 mV/V (especially in the NE sector, near piezometer 2). These anomalies are atypical for granite, but similar chargeabilities have been described in other areas for leachates in industrial waste lands (Deceuster and Kaufmann 2012), in a mine waste rock pile (Power et al. 2018), and related to the dispersion of Pb and Zn in coastal sediments (Puttiwongrak et al. 2019). In the Adaro tailings pond, these values are explained by the percolation of leachates from sulfide minerals in the altered granites underlying the pond.

At greater depths, in both ends of the pond, the chargeabilities increased much more than in previous cases (they can exceed 25 mV/V). These zones correlated with the aforementioned decreases in resistivity (compare Fig. 3b, c). As in other sectors (Martínez et al. 2019; Moreira et al. 2014), this electrical behaviour was interpreted as reflecting metallic mineralisation of the subsoil, which is consistent with the geological context of the sector. The presence of other mining shafts outside the Adaro vein (see Fig. 2a) suggests the existence of secondary veins in the subsoil, which may extend beneath the study pond.

Hydrochemistry

The waters of the Guadiel River have high EC values throughout the mining district, which reflect the significant degree of mineralisation of its waters. Hidalgo et al. (2006) determined a mean value of 845 µS/cm for the surface waters of this sector. In general, this value increases slightly as the river crosses the mining district from the numerous tailings impoundments found near the stream, which affecting the water quality. In March 2019, on the dates when geophysical prospecting campaigns were conducted, the EC of the river water was 833 µS/cm (S3 in Table 1). The research team has been sampling the riverbed periodically, for more than 15 years, which makes it possible to affirm that the chemical water quality of the Guadiel River has improved to some extent since the ponds were encapsulated (Cortada et al. 2017). However, the average Se and Pb concentrations remain above the annual average (AA) value for the environmental quality standards of the European Union normative for surface waters (Table 1). Fe and Mn also reach high values for surface waters (252 µg/L and 879 µg/L, respectively, Table 1) in recent samplings. These results may indicate that, despite the remediation work conducted, leachates are still generated locally in some rainy seasons, which can be incorporated into the riverbed.

With regard to groundwater derived from fractured granite zones unaffected by mining, Hidalgo et al. (2006) found EC values of ≈ 400–500 µS/cm and low metal(loid) concentrations. In the Adaro sector, the waters collected from borehole S1, located upstream of the tailings pond, were analysed. Figure 4 shows the EC and pH values recorded in the water column, which imply the existence of two hydrochemical zones. In the upper section, associated with sedimentary fill and the top layers of altered granite, the water has low EC values (≈ 400 µS/cm), and is apparently unaffected by mining. From 48 m, the zone of fractured granite, the EC values increase moderately, nearing 600 µS/cm. Table 1 presents the physico-chemical characteristics of the waters in the shallow (sample S1a) and deep (sample S1b) zones of the borehole. The waters show a calcium bicarbonate facies, with moderate increases in SO_4^{2-}, HCO_3^{2-}, and Ca concentrations in the bottom section of the borehole. The concentrations of trace elements are very low throughout the water column, typical of waters unaffected by mining in the saturated zone of the hydrogeological system.

The results differ in waters derived from pumping flooded mines. For example, in the Adaro mine shaft (S4 in Table 1) the waters are calcium sulfate-bicarbonate types, with higher Cr, Cu, Fe, Pb, Sr, and Zn concentrations than those recorded in the water from borehole S1. The increased

Table 1 Physico-chemical characteristics of surface and ground waters

	S1a	S1b	S2	S3	S4
EC (µS/cm)	390	580	1423	833	932
Temperature (°C)	19.8	21.0	20.2	15.7	18.6
pH	6.80	7.20	7.09	7.62	7.2
Major constituents (mg/L)					
Ca^{2+}	45	66	178	86	102
Mg^{2+}	12	17	54	24	28
Na^{+}	32	34	52	48	45
K^{+}	1.8	2	20	6	3
Cl^{-}	29	32	94	72	45
SO_4^{2-}	26	36	410	86	126
HCO_3^{-}	134	236	204	236	337
Trace elements (µg/L)					
Al	8	27	275	19	29
As (50 µg/L AA)	8	18	4	11	13
Ba	137	204	62	186	137
Co	0.3	0.1	7.2	1.2	0.4
Cr (50 µg/L AA)	2.4	0.6	1.5	0.7	10
Cu (5-40 µg/L AA)	9.4	4.1	8	5	15
Fe	314	219	384	252	324
Mn	9	18	123	879	21
Pb (7,2 µg/L AA)	5	**16**	**53**	**10**	**47**
Se (1 µg/L AA)	0.4	**1.2**	0.9	**1.2**	**2.6**
Sr	169	288	294	285	460
Zn (30-300 µg/L AA)	103	148	110	47	189
Li	113	84	107	26	–

Sample locations shown in Fig. 1b. Maximum allowable annual average (AA) values for selected elements are included. Contents exceeding the AAs are in bold. *EC* electrical conductivity

sulfate and metallic element contents in this hydrogeological context is linked to the oxidation of sulfides in the flooded mining galleries (Hidalgo et al. 2010).

At piezometer S2, located near the restored Adaro pond, the conductivity was high (1423 µS/cm), in line with the high sulfate content recorded in all waters of this sector (410 mg/L, Table 1). In addition, the concentrations of metallic elements, such as Fe (384 µg/L), Zn (110 µg/L), and Pb (53 µg/L), are significant. The net sulfate facies of this water contrasts sharply with the bicarbonate type of both the water in borehole S1 and the river water (S3). Water chemistry analysis of the main shaft mine shows that the sulfate content of the piezometer water is more than triple that assessed in the flooded mine. Based on these results, despite the waterproofing work conducted in the spoil tip, water still flows within the flotation sludge, which likely generates leachates that infiltrate the permeable bedrock. In addition, these sulfate hydrofacies are correlated with the moderate increases in chargeability detected by IP in surface zones, under the tailings pond, as previously discussed.

This subsurface flow through altered granite zones can reach the riverbed, whose waters show concentrations of some dissolved metals slightly above the current environmental quality standards. However, as observed in the water samples obtained, this situation is limited to the sector near the tailings pond.

Conclusions

Electrical tomography, combining ERT and IP methods, was applied to inspect a restored tailing pond. Accordingly, the low resistivities (20 Ω m) detected in granite under the pond indicated the presence of intensely fractured zones. These zones would have high secondary permeability, which in turn would allow the development of zones of preferential groundwater circulation.

Conversely, chargeability anomalies were detected by IP. In the first 20 m of depth, low chargeability values were obtained, i.e. generally less than 1 mV/V, and no evidence of sulfide minerals was detected. Only at both ends of the pond does the chargeability increase. The moderately high values (≈8 mV/V), which also correlate with zones of decreased resistivity, are typical of altered granite saturated with highly mineralised water.

The chemical analysis of waters sampled in the saturated zone confirmed the geophysical prospecting results. The hydrochemical study conducted at the piezometer at the lowest part of the tailings pond identified high concentrations of dissolved sulfate, carbonates, and metal(loid)s. The concentrations of Fe, Mn, Pb, Zn, and Se were also notable. These elements are associated with the oxidation of metal sulfides present in tailings pond materials and thus may be related to local leachate generation from the tailings. The presence of the sulfate hydrofacies was supported by the IP anomalies.

Leachate contamination associated with the restored tailings pond was locally detected by geophysical prospecting. These results indicate that the ERT and IP methods are effective for inspection and understanding of encapsulated areas.

Acknowledgements The authors thank CEACTEMA (University of Jaén) for partially financing this work. Careful reviews by anonymous referees, by the Editor-in-Chief (Dr. Kleinmann) and by the Guest Editor (Prof. Fernández-Rubio) substantially improved the manuscript.

References

Aristodemou E, Thomas-Betts A (2000) DC resistivity and induced polarisation investigations at a waste disposal site and its environments. J Appl Geophys 44:275–302

Azcárate JE (1977) Mapa geológico y memoria explicativa de la hoja 905 (Linares), escala 1:50.000. Instituto Geológico y Minero de España, Madrid

Bery A, Saad R, Tonnizam E, Jinmin M, Azwin IN, Mohd O, Nordiana MM (2012) Electrical resistivity and induced polarization data correlation with conductivity for iron ore exploration. Electron J Geotech Eng 17:3223–3337

Binley A, Kemna A (2005) DC resistivity and induced polarization methods. In: Rubin Y, Hubbard SS (eds) Hydrogeophysics. Springer-Verlag, Netherlands, pp 129–156

Blondel A, Schmutz M, Franceschi M, Tichané F, Carles M (2014) Temporal evolution of the geoelectrical response on a hydrocarbon contaminated site. J Appl Geophys 103:161–171

Bundschuh J, Litter MI, Parvez F, Román-Ross G, Nicolli HB, Jean JS, Liu ChW, López D, Armienta MA, Guilherme L, Gomez A, Cornejo L, Cumbal L, Toujaguez R (2012) One century of arsenic exposure in Latin America: a review of history and occurrence from 14 countries. Sci Total Environ 429:2–35

Chopin EIB, Aloway BJ (2007) Trace element partitioning and soil particle characterization around mining and smelting areas at Tharsis, Riotinto and Huelva, SW Spain. Sci Total Environ 373:488–500

Cortada U, Martínez J, Rey J, Hidalgo C (2017) Assessment of tailings pond seals using geophysical and hydrochemical techniques. Eng Geol 223:59–70

Dahlin T, Zhou B (2004) A numerical comparison of 2D resistivity imaging with 10 electrode arrays. Geophys Prospect 52:379–398

De la Torre MJ, Hidalgo MC, Rey J, Martínez J (2012) Mineralogical characterization of tailing dams: incidence of abandoned mining works on soil pollution (Linares, Jaén). Geophys Res Abstr 14: EGU2012:13357

Deceuster J, Kaufmann O (2012) Improving the delineation of hydrocarbon impacted soils and water through induced polarization (IP) tomographies: a field study at an industrial waste land. J Contam Hydrol 136–137:25–42

El Adnani M, Plante B, Benzaazoua M, Hakkou R, Bouzahzah H (2016) Tailings weathering and arsenic mobility at the abandoned Zgounder silver mine, Morocco. Mine Water Environ 35:508–524

Fadele SI, Jatau BS, Abaa SI (2018) Geological and induced polarization geophysical investigations of the quartz-vein gold mineralization in some parts of Ayegunle Sheet 226nw, north central Nigeria. J Environ Earth Sci 8:31–41

García-Fernández JM, Gallego J (2009) Proyecto de clausura y restauración del depósito de procesos de tratamiento de industrias

extractivas abandonado "0905-2-0002". EGMASA, Consejería Medio Ambiente, Junta de Andalucía, Sevilla (unpublished)
Gratton WS, Nkongolo KK, Spiers GA (2000) Heavy metal accumulation in soil and jack pine (Pinus banksiana) needles in Sudbury, Ontario, Canada. Bull Env Contam Toxicol 64:550–557
Griffiths DH, Barker RD (1993) Two-dimensional resistivity imaging and modelling in areas of complex geology. J Appl Geophys 29:211–226
Gutiérrez-Guzmán J (1999) Las minas de Linares. Apuntes históricos. Colegio Oficial de Ingenieros Técnicos de Minas de Linares, Linares
Herbet RB (1997) Partitioning of heavy metals in podzol soils contaminated by mine drainage waters, Dalarna, Sweden. Water Air Soil Poll 96:39–59
Hidalgo MC, Benavente J, El Mabrouki K, Rey J (2006) Estudio hidroquímico comparativo en dos sectores con minas abandonadas de sulfuros metálicos: distrito de Linares-La Carolina (Jaén). Geogaceta 39:123–126
Hidalgo MC, Rey J, Benavente J, Martínez J (2010) Hydrogeochemistry of abandoned Pb sulphide mines: the mining district of La Carolina (southern Spain). Environ Earth Sci 61:37–46
Irawan D, Sumintadireja P, Saepuloh A (2013) Subsurface imaging techniques for deep ore mineral mapping using geoelectrical and induced polarization (IP) methods. Procedia Earth Planet Sci 6:139–144
Ji K, Kim J, Lee M, Park S, Kwon HJ, Cheong HK, Jang JY, Kim DS, Yu S, Kim YW, Lee KY, Yang SO, Jhung IJ, Yang WH, Paek H, Ch Hong Y, Choi K (2013) Assessment of exposure to heavy metals and health risks among residents near abandoned metal mines in Goseong, Korea. Environ Poll 178:322–328
Li X, Thornton I (2001) Chemical partitioning of trace and major elements in soils contaminated by mining and smelting activities. Appl Geochem 16:1693–1706
Lillo J (1992) Geology and Geochemistry of Linares-La Carolina Pb-Ore field (southeastern border of the Hesperian Massif). PhD Thesis, Univ of Leeds, UK
Lindsay MBJ, Moncur MC, Basin JG, Jambor JL, Ptacek CJ, Blowes DW (2015) Geochemical and mineralogical aspects of sulfide mine tailings. Appl Geochem 57:157–177
Loke MH (2014) Tutorial: 2-D and 3-D electrical imaging surveys, Revision date: 5th Nov 2014. www.geotomosoft.com (ACCESSED 2015-02-19)
Loke MH, Barker RD (1996) Rapid least-squares inversion of apparent resistivity pseudosections by a quasi-Newton method. Geophys Prospect 44:131–152
Loke MH, Dahlin T (2002) A comparison of the Gauss-Newton and quasi-Newton methods in resistivity imaging inversion. J Appl Geophys 49:149–162
Martín-Crespo T, Gómez-Ortíz D, Martín-Velázquez S, Esbrí JM, De Ignacio-San José C, Sánchez-García MJ, Montoya-Montes I, Martín-González F (2015) Abandoned mine tailings in cultural itineraries: Don Quixote Route (Spain). Eng Geol 197:82–93
Martínez J, Llamas J, De Miguel E, Rey J, Hidalgo MC (2008) Determination of geochemical background in a metal mining site: example of the mining district of Linares (South Spain). J Geochem Explor 94:19–29
Martínez J, Rey J, Hidalgo C, Benavente J (2012) Characterizing abandoned mining dams by geophysical (ERI) and geochemical methods: the Linares-La Carolina District (southern Spain). Water Air Soil Poll 223:2955–2968
Martínez J, Hidalgo MC, Rey J, Garrido J, Kohfahld C, Benavente J, Rojas D (2016) A multidisciplinary characterization of a tailings pond in the Linares-La Carolina mining district, Spain. J Geochem Explor 162:62–71
Martínez J, Rey J, Sandoval S, Hidalgo C, Mendoza R (2019) Geophysical prospection using ERI and IP techniques to locate vein deposits. Remote Sens Basel. https://doi.org/10.3390/rs11242923
Martínez-Pagán P, Faz Cano A, Aracil E, Arocena JM (2009) Electrical resistivity imaging revealed the spatial properties of mine tailing ponds in the Sierra Minera of Southeast Spain. J Environ Eng Geophys 14:63–76
Moncur MC, Ptacek CJ, Blowes DW, Jambor JL (2005) Release, transport and attenuation of metals from an old tailings impoundment. Appl Geochem 20:639–659
Moreira CA, Rezende Borges M, Lira Vieira G, Malagutti Filho W, Fernándes Montanheiro M (2014) Geological and geophysical data integration for delimitation of mineralized areas in a supergene manganese deposits. Geofísica Int 53:199–210
Navarro A, Font X, Viladevall M (2015) Metal mobilization and zinc-rich circumneutral mine drainage from the abandoned mining area of Osor (Girona, NE Spain). Mine Water Environ 34:329–342
Nordstrom DK, Blowes DW, Ptacek CJ (2015) Hydrogeochemistry and microbiology of mine drainage: an update. Appl Geochem 57:3–16
Power Ch, Tsourlos P, Ramasamy M, Nivorlis A, Mkandawire M (2018) Combined DC resistivity and induced polarization (DC-IP) for mapping the internal composition of a mine waste rock pile in Nova Scotia, Canada. J Appl Geophys 150:40–51
Puttiwongrak A, Suteerasak T, Mai PhK, Hashimoto K, Gonzalez JC, Rattanakom R, Prueksakorn K (2019) Application of multi-monitoring methods to investigate the contamination levels and dispersion of Pb and Zn from tin mining in coastal sediments at Saphan Hin, Phuket, Thailand. J Clean Prod 218:108–117
Rojas D, Benavente J, Hidalgo MC, Rey J, Martínez J (2012) Contenido total y fraccionamiento de metales y semimetales en las escombreras del distrito minero de Linares-La Carolina (Jaén). Geotemas 11:1495–1498
Sasaki Y (1992) Resolution of resistivity tomography inferred from numerical simulation. Geophys Prospect 40:453–464
Schwartz N, Furman A (2012) Spectral induced polarization signature of soil contaminated by organic pollutant: experiment and modeling. J Geophys Res 117:B10203
Slater LD, Lesmes D (2002) I.P. interpretation in environmental investigations. Geophysics 67:77–88
Sobanska S, Ledésert B, Deneele D, Laboudigue A (2000) Alteration in soils of slag particles resulting from lead smelting. CR Acad Sci II 33(1):271–278
Sumner JS (1976) Principles of induced polarization for geophysical exploration. Elsevier Scientific Publishing, Amsterdam
Telford WM, Geldart LP, Sheriff RE (1990) Applied geophysics. Cambridge University Press, Cambridge
Towel JN, Anderson RG, Pelton WH, Olhoeft GR, Labrecque D (1985) Direct detection of hydrocarbon contaminants using induced polarization method. In: SEG meeting, pp 145–147
Yun SW, Baveye PhC, Kim KB, Kang DH, Lee SY, Son J, Kim DH, Yoon Y, Yu Ch (2016) Effect of postmining land use on the spatial distribution of metal(loid)s and their transport in agricultural soils: analysis of a case study of Chungyang, South Korea. J Geochem Explor 170:157–166
Zarroca M, Linares R, Velásquez-López PC, Roqué C, Rodríguez R (2015) Application of electrical resistivity imaging (ERI) to a tailings dam project for artisanal and small-scale gold mining in Zaruma–Portovelo, Ecuador. J Appl Geophys 113:103–113
Zhadanov MS (2018) Direct current and induced polarization methods. In: Ch 12 in Foundations of Geophysical Electromagnetic, Theory and Methods, 2nd edit, Elsevier, pp 439–493